CHANDRA
X-ray Center   60 Garden St., Cambridge Massachusetts 02138 USA

Chandra X-ray Observatory revolutionized the X-ray astronomy as being the first, and so far the only, X-ray telescope achieving sub-arcsecond resolution. Chandra comprises of three principal elements: the High Resolution Mirror Assembly (HRMA), Pointing Control and Aspect Determination (PCAD) system, and the Science Instrument Module (SIM). To achieve and retain the unprecedented imaging quality, it is critical that these three principal elements stay rigid and stable for the entire life time of the Chandra operation. Measuring and tracking the telescope optical axis and aimpoint positions are the key to understand the stability of the telescope and to maintain the optimal Chandra operation.

1   Definitions

Let's first give the following definitions:

- Focal-Point: Point on the focal plane where the sharpest PSF is located.

- Optical Axis: Axis perpendicular to the focal plane at the focal-point.

- Aimpoint: Point on the focal plane where the image of a source with zero Y and Z offsets is located.

For ideal Wolter-I mirror pairs, the optical axis is the mathematical axis of both paraboloid and hyperboloid mirror surfaces, and it passes through both focal-point and aimpoint on the focal plane, i.e. the focal-point and aimpoint are the same. For the actual HRMA, the focal-point and aimpoint are close but not identical. The origin of the Y and Z offsets was set before the launch, with the best estimate at the time to match the aimpoint and optical axis positions. This origin has never changed.

2   Telescope Pointing

The telescope pointing, i.e. the target acquisition, is accomplished through the following steps (refer POG Figure 5.3):

1. Target coordinate: the target coordinate is requested by the observer, which is registered as (RA_targ, Dec_targ) in the data header.

2. ACA attitude (Aspect Camera Assembly pointing): based on the target coordinate (RA_targ, Dec_targ), the ACA pointing (command position) is computed in terms of quaternions, which are registered in the ACA database. There is an $89.6''$ offset between the target position and ACA pointing, due to the pre-launch ACA alignment.

3. Telescope attitude (HRMA pointing): once the ACA is pointed to its command position, the HRMA is automatically pointed to (RA_pnt, Dec_pnt), which is the computed mean pointing of the (dithered) observation. This information is registered in the data header. There is a $\sim 97''$ offset between the HRMA pointing and the ACA pointing.

4. Target position: once the HRMA is pointed to (RA_pnt, Dec_pnt), the image of an onaxis target will be at the aimpoint[1], which has the requested coordinates (RA_targ, Dec_targ). There is a $\sim 17''$ offset between (RA_pnt, Dec_pnt) and (RA_targ, Dec_targ).

3   Aimpoint on Chandra Detectors

For each Chandra observation. one of four Chandra detectors is aligned with the optical axis by moving the entire SIM to that detector's nominal SIM-Z position. Figure 1 shows the Chandra detectors layout in the SIM plane and the aimpoint locations with their nominal SIM-Z positions.

4   Aimpoint and Optical Axis Drifts

Both the aimpoint and the optical axis have been drifting in the SIM plane since launch. Their relative positions are changing constantly. Their positions on each detector are critical for the optimal operation of the Chandra X-ray Observatory. Therefore the positions of both points are continuously monitored.

4.1   Aimpoint Drift

Since launch, the Chandra aimpoint has been drifting in the SIM $[-Y, -Z]$ direction. Figures $2 - 5$ show the aimpoint (with zero offset) positions of all the Chandra observations with nominal SIM-Z positions on all four detectors in chip coordinates as a function of time since launch. It is seen that the aimpoint is drifting in the SIM $[-Y, -Z]$ direction from 1999 until the beginning of year 2011. The two sudden large jumps in June 2003 and November 2006 are due to the ACA cool-down. In early 2011, the aimpoint drift reversed its direction, especially after the safemode in July 2011. In early 2012, the aimpoint drift is reversed again, back to its original trend in the SIM $[-Y, -Z]$ direction. Note that there appears to be an increasing trend in the short-term fluctuations of the aimpoint position.

4.2   Optical Axis Drift

Unlike the aimpoint, the drift of the optical axis does not exhibit any particular trend. The optical axis position is derived from data obtained on annual raster scan observations of Ar Lac with the HRC-I. The HRC-I is the only detector for which the optical axis is directly measured. Figure 6 shows the scan data points taken in September 2012. The five circles around each data point indicate the 50%, 60%, 70%, 80% and 90% encircled energies. For clarity, the circle radii are 5 times the actually encircled energy radii. The optical axis is determined by fitting the radii to 2-dimensional quadratic functions in detector coordinates. By definition, the optical axis is at the point where the quadratic function at its minimum. Figure 7 shows the optical axis derived from the above 2-D quadratic fit. Figure 8 shows all the optical axis positions so determined since launch. It moves like a random walk but is relatively stable. Its movement is well within a $10''$ region. Since year 2003, the optical axis drift was only in a $5''$ region.

---

[1]Since the Chandra spacecraft has a built-in dither (of Lissajous figure with peak-to-peak amplitude of $16''$ for ACIS and $40''$ for HRC) on its pointing position to average across calibration uncertainties, the aimpoint is actually the center of the dither pattern.
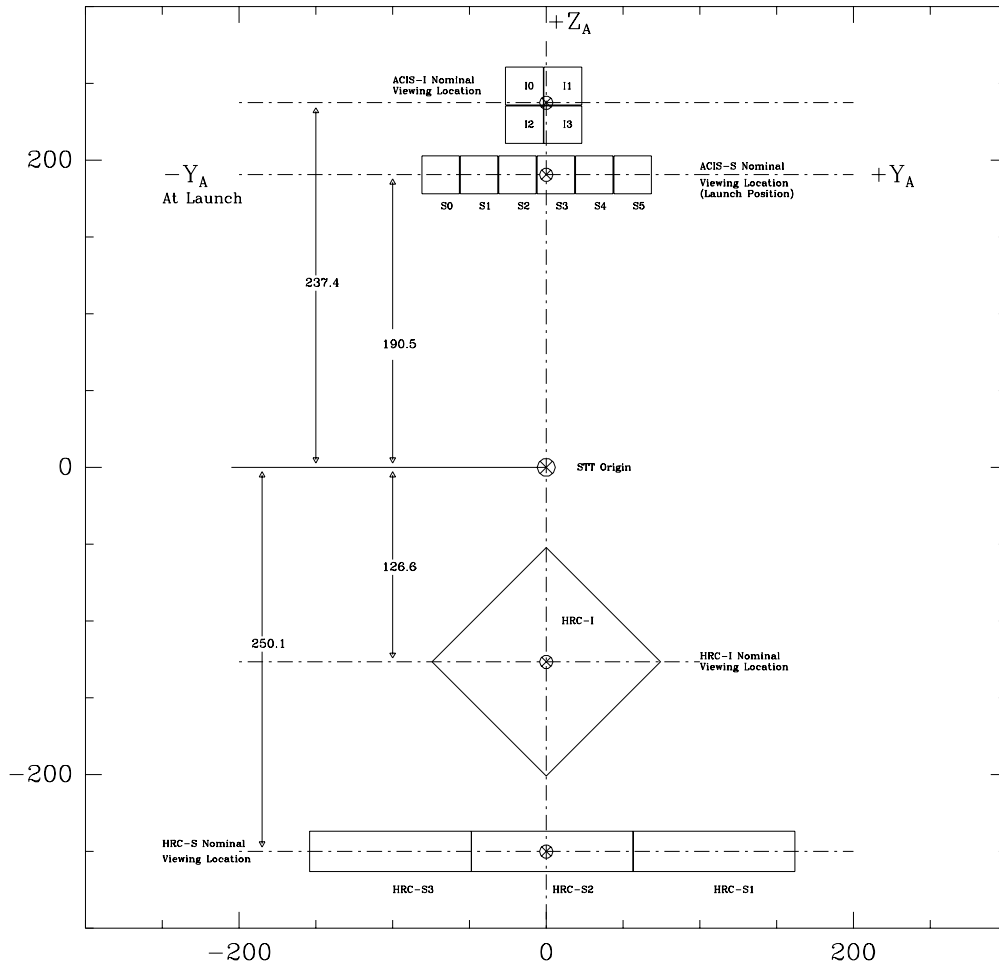
Figure 1: Chandra Detectors Layout: The SIM Translation Table shows the flight focal plane instrument to scale (in mm, coordinate system is AXAF-STT-1.0). SIM +Y is along the x-axis; SIM +Z is along the y-axis. ⊗ on each detector marks the aimpoint position with nominal SIM-Z position and zero pointing offset.
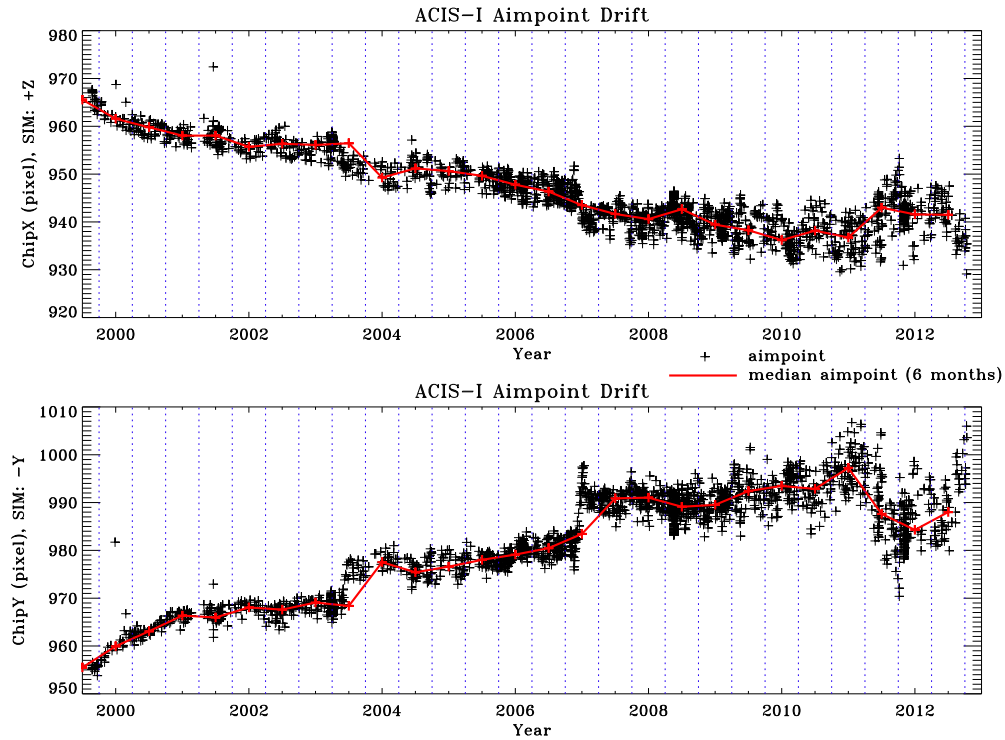
Figure 2: Aimpoint position as a function of time on ACIS-I. Solid red lines show the median aimpoint drift in 6 months bins, which are separated by vertical dotted blue lines.
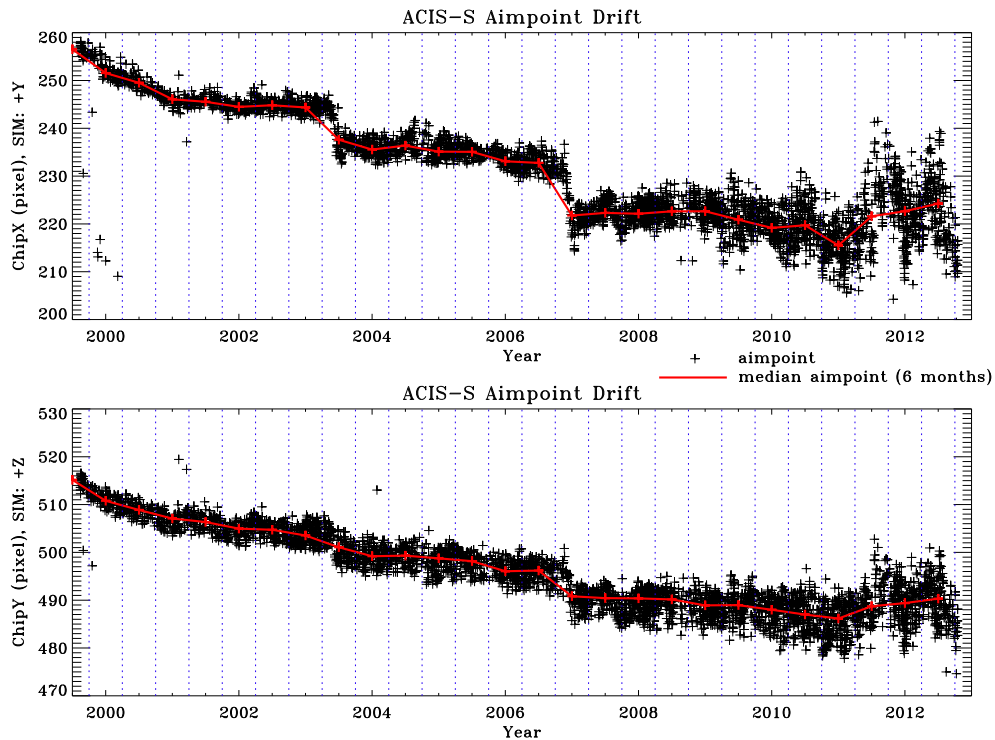

Figure 3: Aimpoint position as a function of time on ACIS-S. Solid red lines show the median aimpoint drift in 6 months bins, which are separated by vertical dotted blue lines.
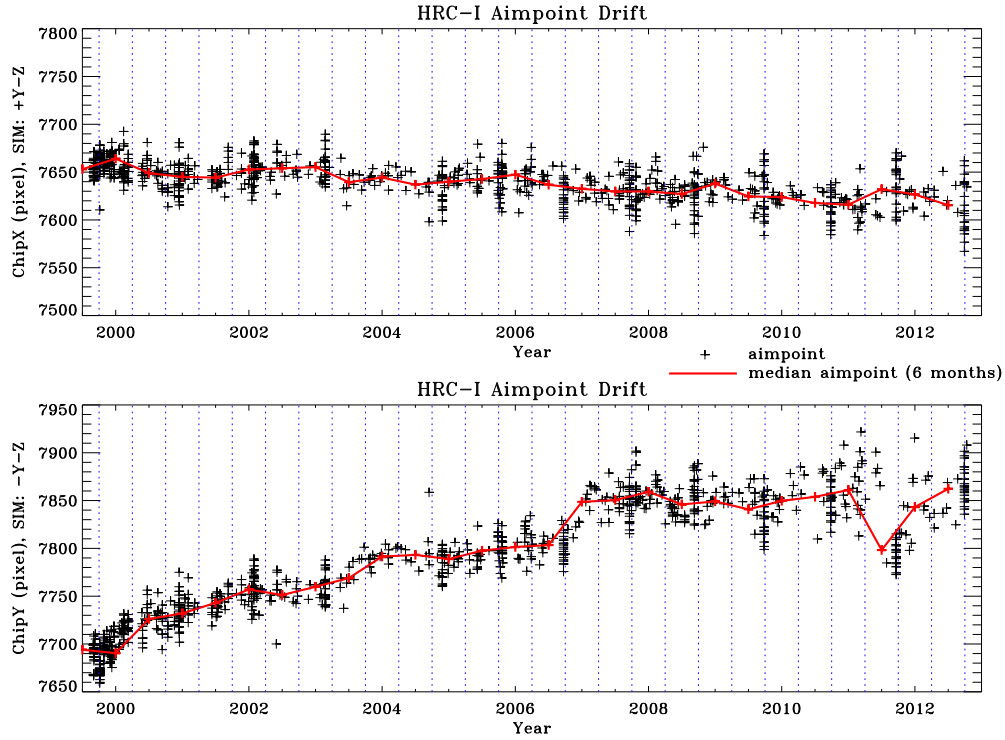
Figure 4: Aimpoint position as a function of time on HRC-I. Solid red lines show the median aimpoint drift in 6 months bins, which are separated by vertical dotted blue lines.
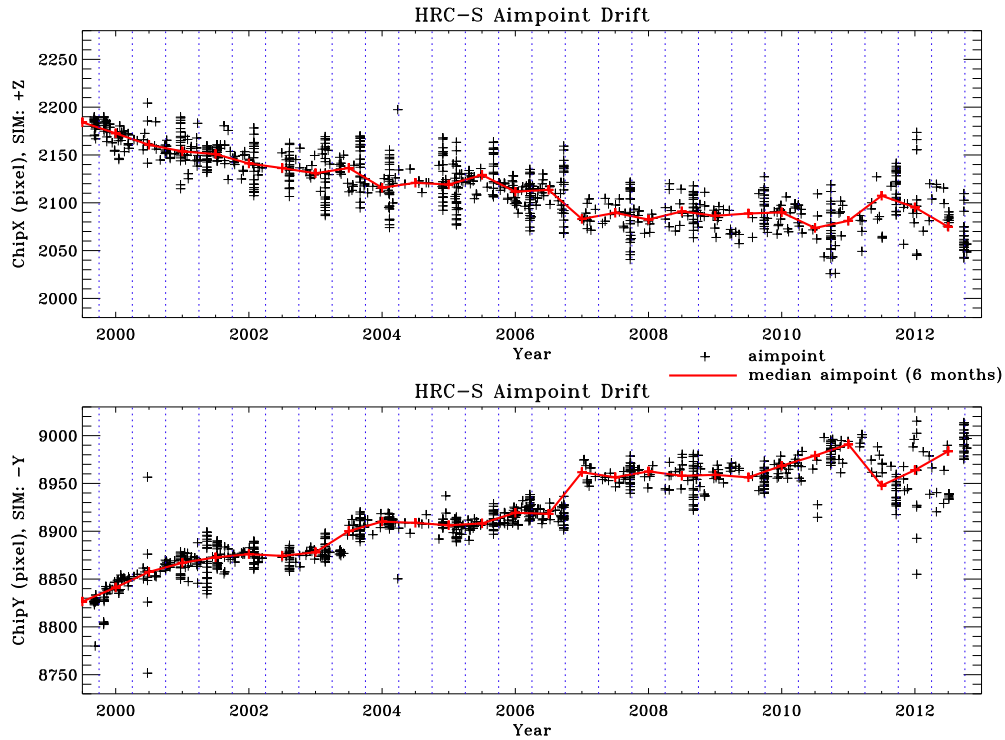

Figure 5: Aimpoint position as a function of time on HRC-S. Solid red lines show the median aimpoint drift in 6 months bins, which are separated by vertical dotted blue lines.
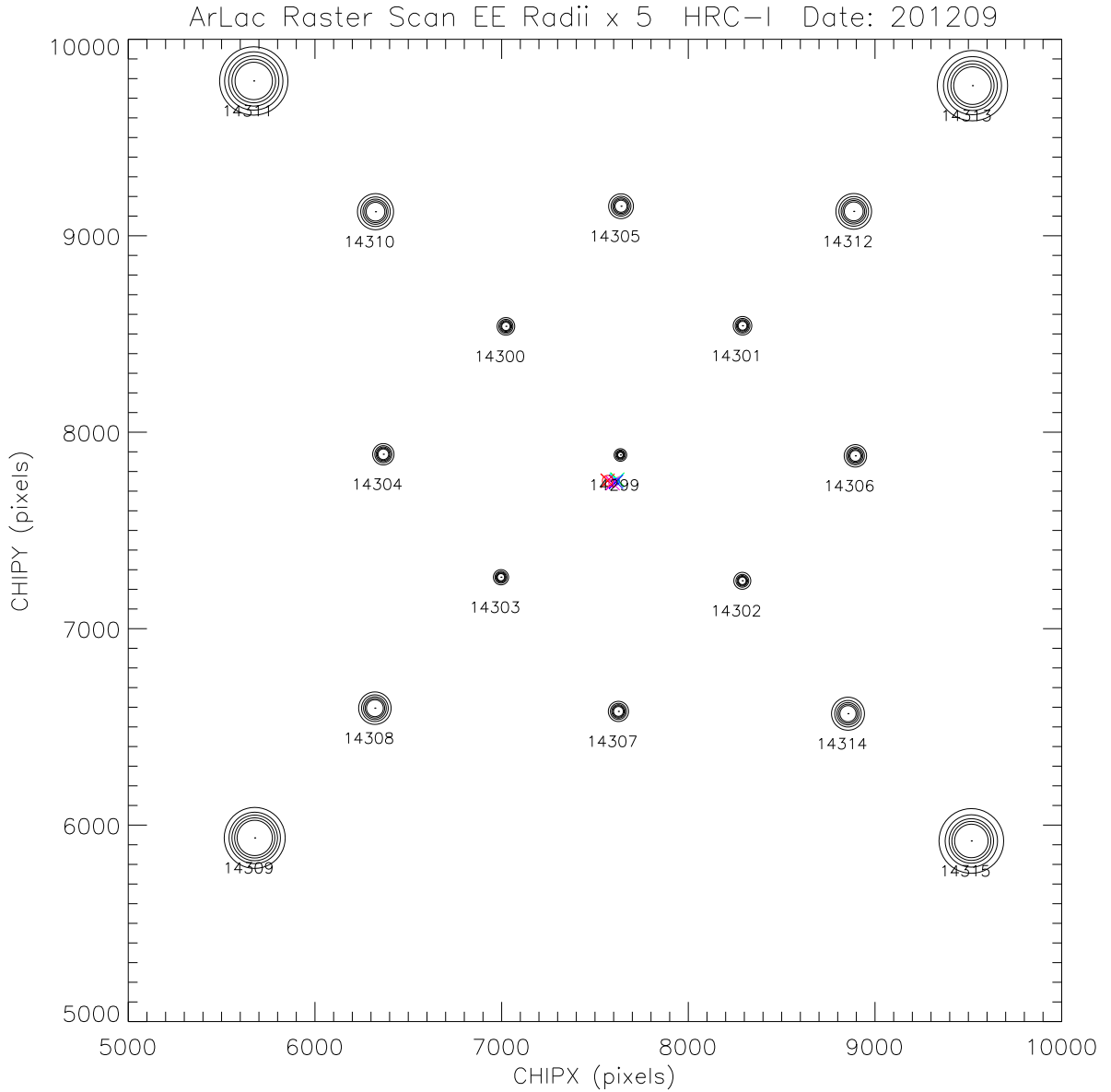
Figure 6: HRC-I raster scan observation of Ar Lac in chip coordinates. Circles around each observation point have the 50% – 90% encircled energy radii × 5. The data are fit to a 2-D quadratic function to find the optical axis. Data taken in September 2012. The numbers under the circles are OBSIDs of the observations.
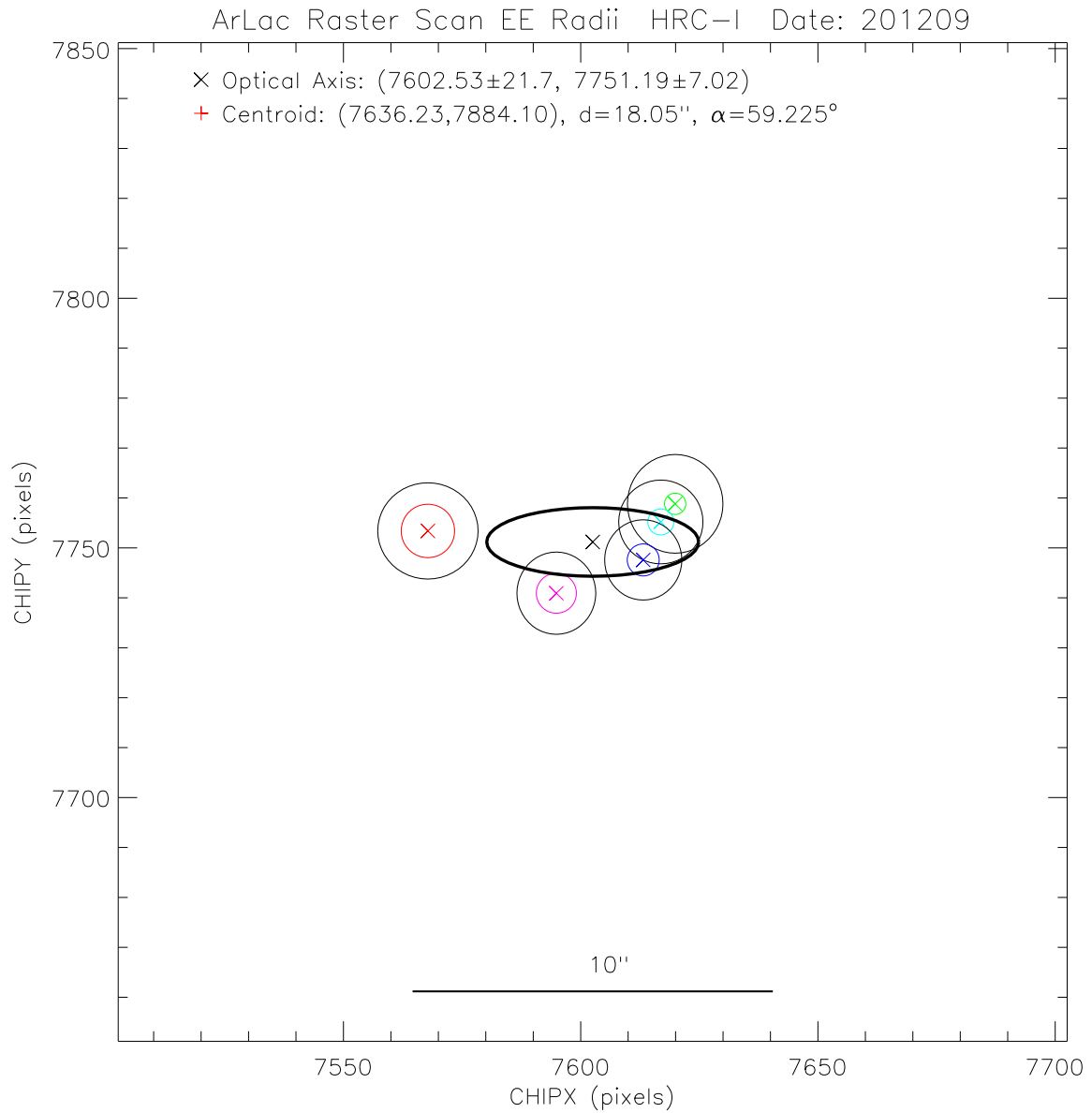
Figure 7: Same as Fig. 6 but zoomed in to the optical axis region. The five colored ×'s are the positions of quadratic function minimum for 50% – 90% encircled energy fit. The colored circles indicate their encircled energy radii. The black circles are the 1-σ fit errors. The black × marks the optical axis position, taken as the mean of the above 5 minimums. The black oval is the 1-σ error ellipse.
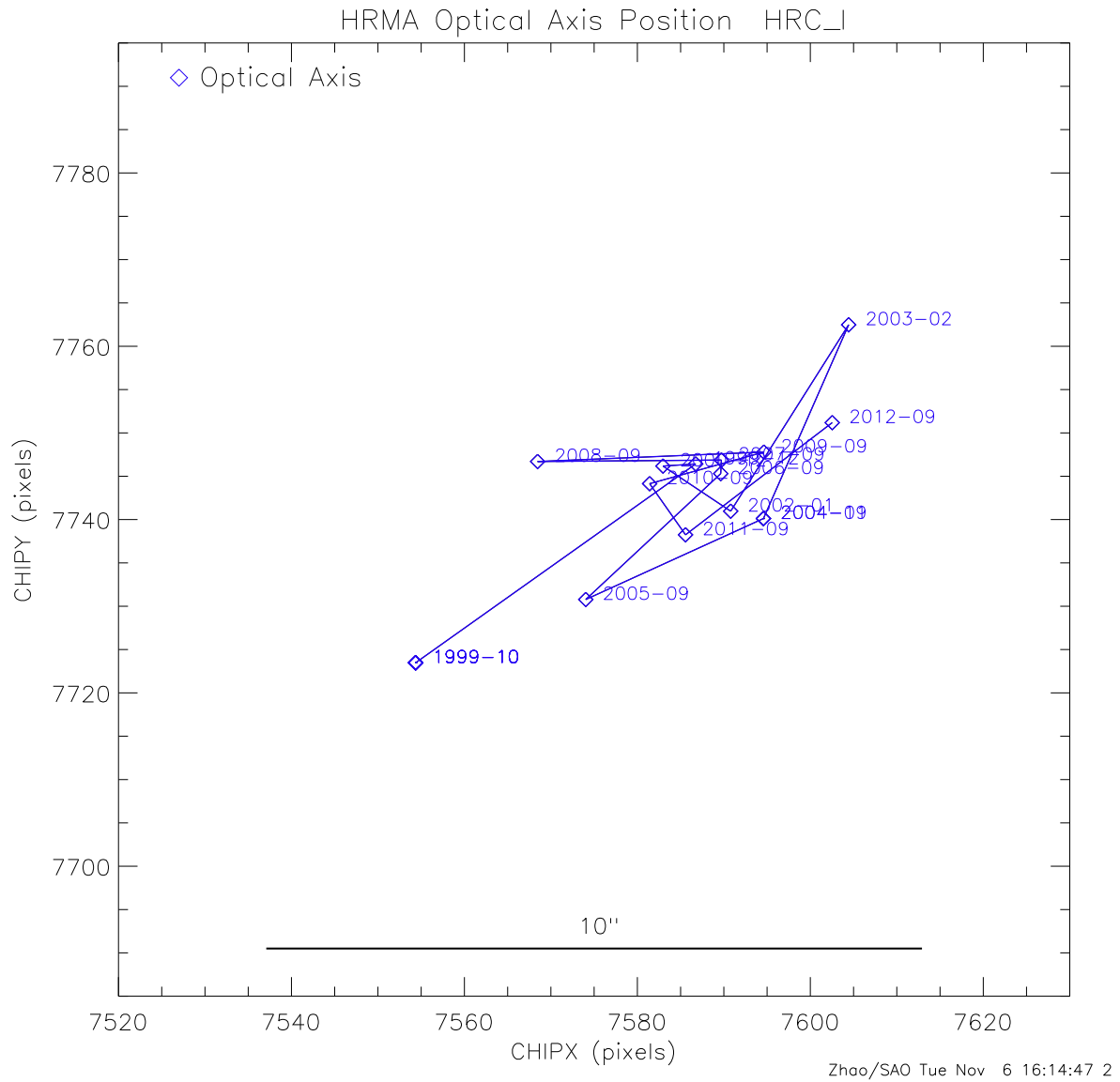
Figure 8: Chandra optical axis positions on HRC-I since launch. Each position is labeled by the year–month. The position is relatively stable and well with in a $10''$ region.

5   Aimpoint and Optical Axis on Detectors

Aimpoint positions are measured on all four detectors as described in Section 4.1. The optical axis positions are measured only on HRC-I as described in Section 4.2. However, at any given time, the relative position between the aimpoint and optical axis is the intrinsic property of the HRMA and ACA, independent of the detectors. One can therefore calculate the optical axis position on other detectors based on its relative position to the aimpoint.

Figures 9 and 10 show the optical axis and aimpoint positions on HRC-I and HRC-S. The blue diamonds show the optical axis positions. The red arrows show the aimpoint position drift. While the optical axis is relatively stable, the aimpoint has been drifting in the SIM $[-Y, -Z]$ direction since launch until early 2011, for about $25''$. Then it reversed its drift direction, especially after the safemode in July 2011. In early 2012, the aimpoint drift is reversed again, back to its original trend in the SIM $[-Y, -Z]$ direction.

Figures 11 shows the optical axis and aimpoint positions on ACIS-I. The green arrow in the Figure indicates a default offset that is applied (see Section 6 for more details). Since December 2006, all the ACIS-I observations have been conducted with this default offset, unless the observers requested otherwise.

Figures 12 shows the optical axis and aimpoint positions on ACIS-S. Because of the aimpoint drift, four different default offsets have been implemented in order to avoid the dither pattern falls on the node boundary 0|1. These are indicated by the green arrows in the figure (see Section 6 for more details).

Figure 9: Chandra optical axis (blue) and median aimpoint (red, see Fig. 4) positions on HRC-I. Each aimpoint position is labeled by the year. The cyan colored arrows show the SIM directions.
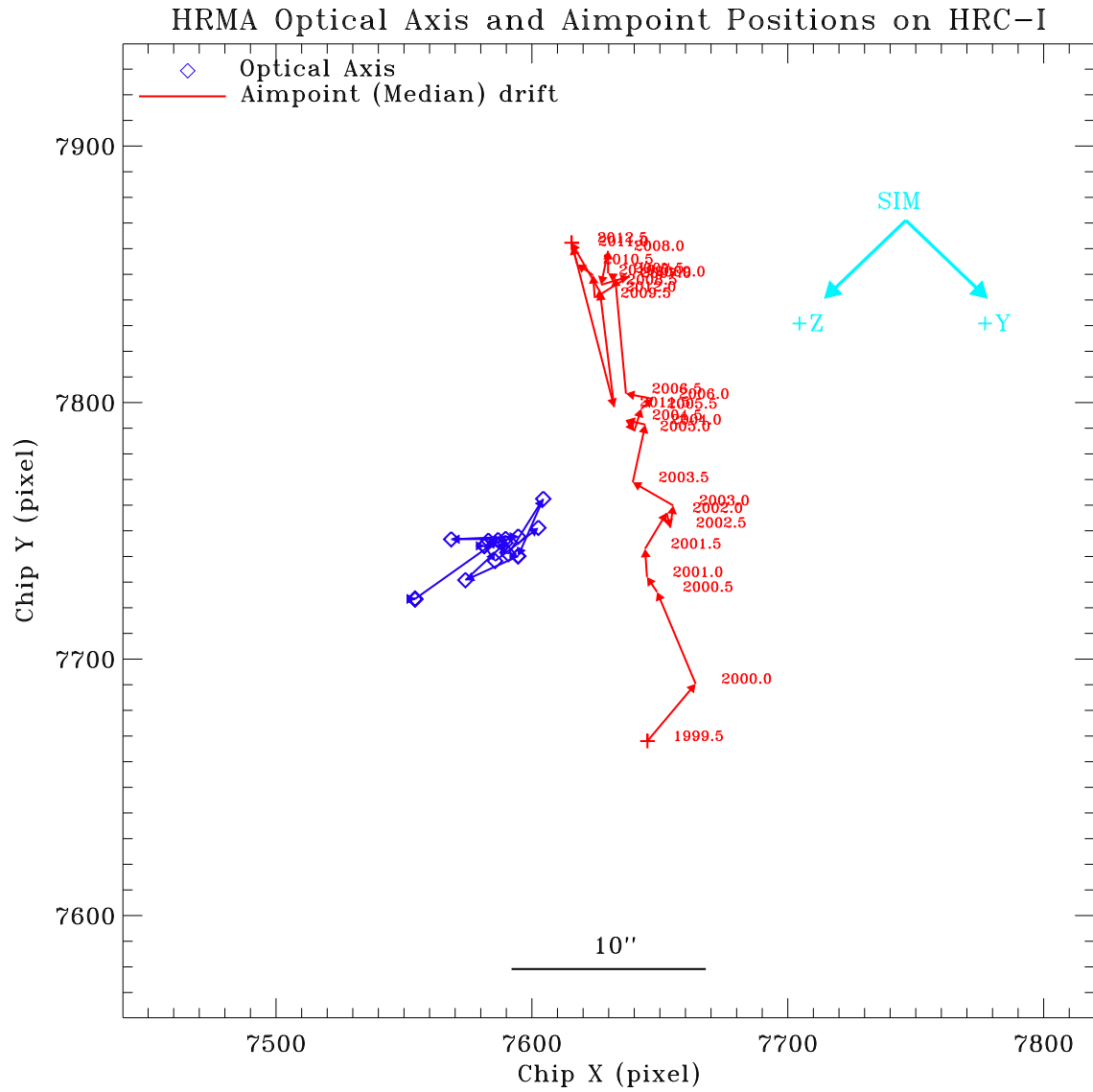
Figure 10: Chandra optical axis (blue) and median aimpoint (red, see Fig. 5) positions on HRC-S. Each aimpoint position is labeled by the year. The cyan colored arrows show the SIM directions.

Figure 11: Chandra optical axis (blue) and median aimpoint (red, see Fig. 2) positions on ACIS-I. Each aimpoint position is labeled by the year. The cyan colored arrows s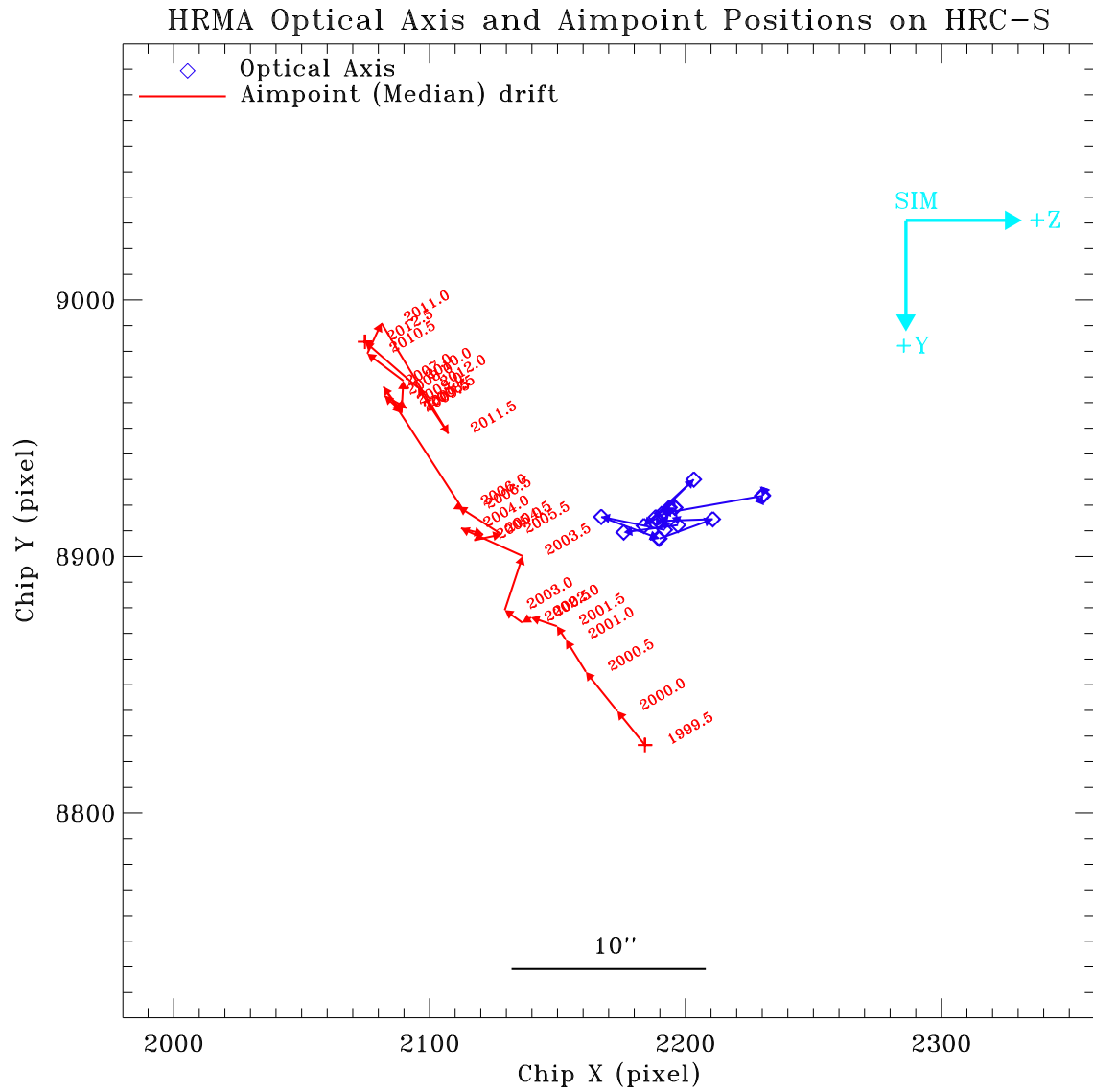how the SIM directions. ACIS-I observations were conducted without default offset since launch until the end of 2006. In December 2006, the aimpoint had a sudden shift of $\sim 10''$ due to the ACA primary focal plan CCD cool down from $-15°$C to $-20°$C. This sudden shift brought the aimpoint uncomfortably close to the ACIS-I3 chip boundary. As it continue to drift towards the boundary, the dither pattern ($16''$ peak-to-peak) will soon fall out of the chip. Therefore a default Y-offset $= -15''$ and Z-offset $= -12''$ was implemented to move the aimpoint away from the chip boundary and also closer to the optical axis. The green arrow shows the magnitude and the direction of this default offset. Since then, all the ACIS-I observations have been conducted with this default offset, unless the observers requested otherwise.
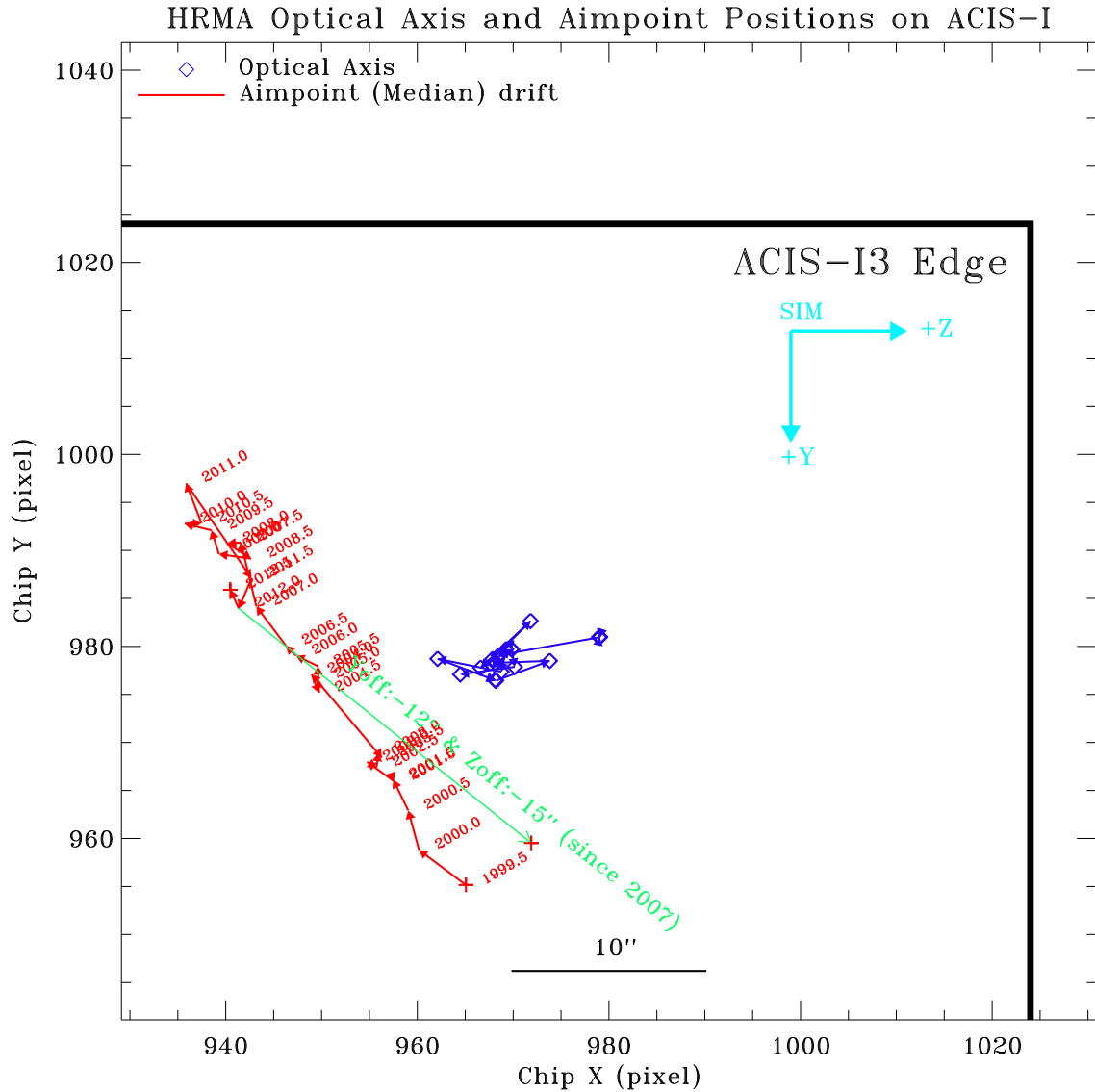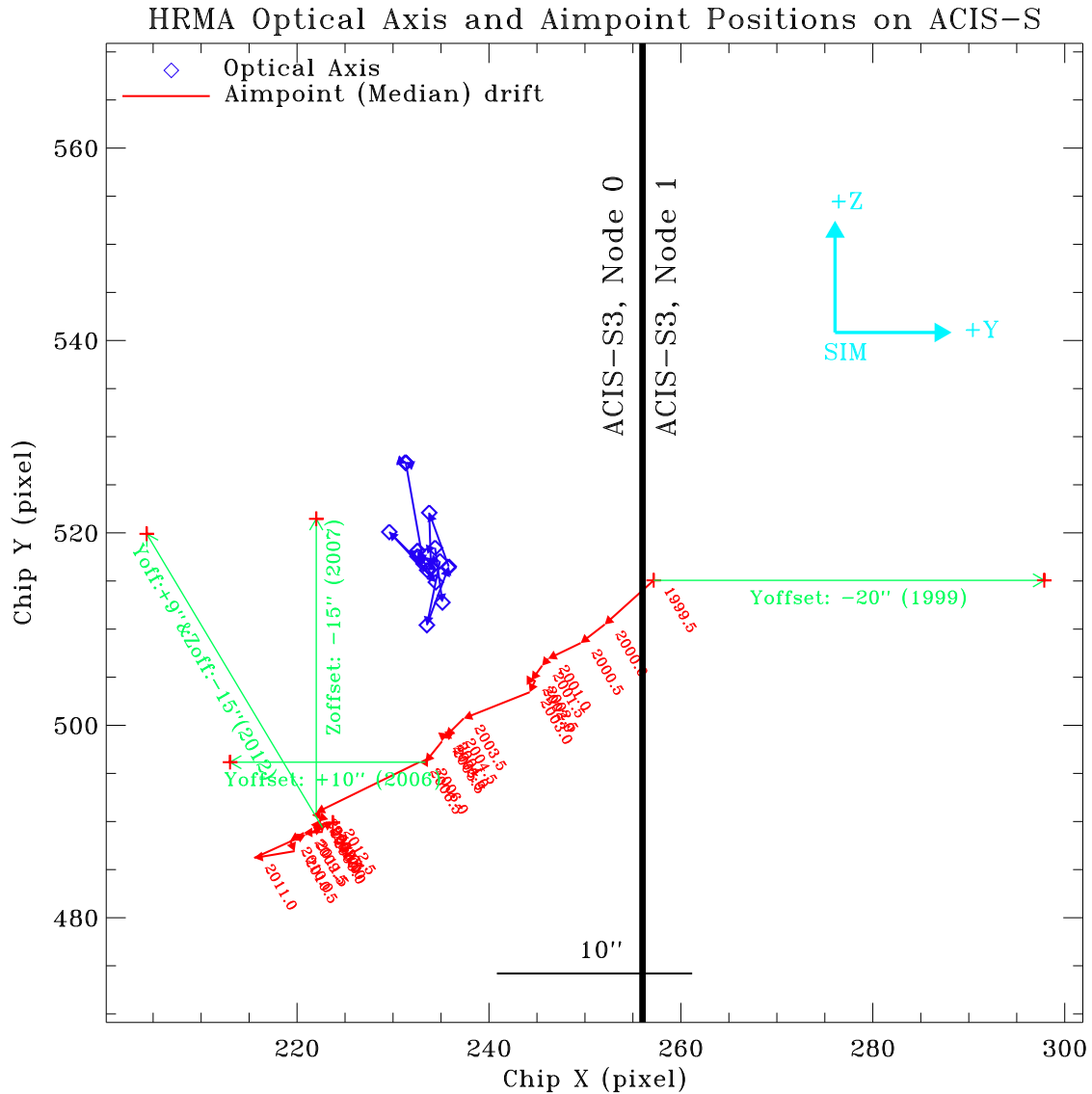
Figure 12: Chandra optical axis (blue) and median aimpoint (red, see Fig. 2) positions on ACIS-S. Each aimpoint position is labeled by the year. The cyan colored arrows show the SIM directions. The green arrows show the default offsets implemented over the years (see Section 6 for more details).

6 Aimpoint Default Offsets

It is not desirable for the aimpoint to be too close to a detector edge, an ACIS chip or node boundary. In order to avoid the dithered image from crossing such boundaries, default pointing offsets were applied on ACIS detectors. Since the aimpoint has been drifting, the default offset has been adjusted accordingly during the course of Chandra operation. Table 1 summarizes these default offset implementations on ACIS-I and ACIS-S. They are illustrated in Figures 11 and 12 with green arrows.

Table 1: Default Offsets on ACIS Detectors

Detector	Date Applied	Y-offset	Z-offset	Reason
ACIS-I	1999 Aug.	0.0	0.0	No offset applied.
	2006 Dec.	$-12''$	$-15''$	Move the aimpoint away from the I3 edge
				& closer to optical axis.
ACIS-S	1999 Aug.	$-20''$	0.0	Move the aimpoint away from node 0|1
	2005 Dec.	$+10''$	0.0	Move the aimpoint away from node 0|1
	2006 Dec.	0.0	$-15''$	Move the aimpoint closer to optical axis.
	2011 Aug.	$+9''$	$-15''$	Move the aimpoint away from node 0|1
				& closer to the optical axis.

The aimpoints on HRC-I and HRC-S are well within the center region of both detectors. Thus there are no default offset ever needed for HRC detectors.

7 Impact on Chandra Observations

Because the optical axis position has been relatively stable (as shown in Section 4.2), the HRMA PSF and therefore the superb Chandra imaging resolution has stayed the same since launch.

Given the aimpoint has been drifting and appropriate default offsets have been implemented to compensate the drift (see Section 6), the relative positions of the optical axis and aimpoint has been changing, but at no time they were more than $20''$ apart. Since this is relatively small comparing to the offaxis angle at which the PSF starting to degrade (See POG Figures 4.12 and 4.13), the PSF of near axis sources has always stayed the same during the Chandra operation.

8 Current Optical Axis and Aimpoint positions

Each October, a new table of optical axis and aimpoint positions are compiled for the new release of Chandra POG (Proposers' Observatory Guide), CIAO (Chandra Interactive Analysis of Observations) and ObsVis (The Chandra Observation Visualizer).

The Chandra Cycle 15 optical axis and aimpoint positions are listed in Table 2. On-axis targets will be imaged at the aimpoint (with the default offsets for ACIS-I and S) chip coordinates on each detector. Observers should use this table to check their target location and may request different pointing offset based on their sources to maximize the scientific return. If no pointing offset is specified, the default offset will be applied.

Table 2: Chandra Optical axis and aimpoint Positions for Cycle 15

Detector	SIM-Z (mm)	Optical Axis ChipX	ChipY	Aimpoint ChipX	ChipY	Chip	Default offset
ACIS-I	-233.587	964	977	941	988	I3	none
				972	964	I3	$\Delta Y=-12''$ & $\Delta Z=-15''$
ACIS-S	-190.143	235	513	224	490	S3	none
				206	521	S3	$\Delta Y=+9''$ & $\Delta Z=-15''$
HRC-I	126.983	7603	7751	7615	7862		none
HRC-S	250.466	2176	8909	2075	8984	S2	none

9   Summary

By studying the optical axis and aimpoint, we can understand the long term stability and imaging quality of the telescope and ensure its optimal performance.

The study shows that optical axis position has been relatively stable since launch. Its random walk like movement is well within a $10''$ region. This result indicates that the HRMA, optical bench and SIM are all very rigid and stable. Therefore the superb Chandra spatial resolution has always been the same.

The study shows that the aimpoint has been drifting in the SIM $[-Y,-Z]$ direction for about $25''$. In the past two years the drift has reversed its direction twice. In addition, the short term fluctuation has gradually increased. The aimpoint drift is caused by the alignment change between the ACA and the HRMA. Its long term change is due to the aging and relaxing of the material. Its short term change is usually associated with the thermal change in the ACA housing. So in order to keep the aimpoint stable in short term, we need to keep a constant temperature of the ACA.

Although both optical axis and aimpoint have been drifting since launch, at no time Chandra's imaging quality was effected. We just need to continue monitoring their drifts and adjust the default pointing offsets to avoid the aimpoint getting too close to the chip edge or node boundary.

10   References

Zhao, Ping "Chandra Telescope Optical Axis", Chandra Calibration Workshop, 2004, Cambridge, MA
http://cxc.cfa.harvard.edu/ccw/proceedings/04_proc/presentations/zhao
Zhao, Ping "Chandra Telescope Optical Axis and Aimpoint", Chandra Calibration Workshop, 2005, Cambridge, MA
http://cxc.cfa.harvard.edu/ccw/proceedings/05_proc/presentations/zhao
Zhao, Ping "Chandra Telescope Optical Axis and Aimpoint", Chandra X-ray Center Memorandum, 2006
http://cxc.harvard.edu/cal/Hrma/rsrc/Publish/Optics/OpticalAxisAndAimpoint/opt_axis_memo.pdf
Zhao, Ping "Chandra Telescope Optical Axis and Aimpoint", Chandra Calibration Workshop, 2007, Huntsville AL
http://cxc.cfa.harvard.edu/ccr/proceedings/07_proc/presentations/zhao
Zhao, Ping "The Quality and Stability of Chandra Telescope Pointing and Spatial Resolution", Chandra Calibration Review, 2009 Boston, MA
http://cxc.harvard.edu/ccr/proceedings/2009/presentations/zhao

Zhao, Ping "Chandra Aimpoint Drift and Default Offsets", Chandra X-ray Center Memorandum, 2011
http://cxc.harvard.edu/cal/Hrma/rsrc/Publish/Optics/OpticalAxisAndAimpoint/aimpoint_memo-20111109.pdf
Zhao, Ping "Chandra X-ray Observatory Aimpoint and Optical Axis", AAS 219th meeting, 2012, Bull.Am.Astro.Soc. 219, 446.01
Zhao, Ping "The Quality and Stability of Chandra Telescope Pointing and Spacial Resolution", AAS 220th meeting, 2012, Bull.Am.Astro.Soc. 220, 122.05